D 1.1: Theoretical scheme on how to conduct experiments in circuit QED systems and in systems of trapped ions

Adiabatic quantum simulation with a segmented ion trap: Application to long-distance entanglement in quantum spin systems

S. Zippilli[1], M. Johanning[2], S. M. Giampaolo[1], Ch. Wunderlich[2], and F. Illuminati[1*]

[1]*Dipartimento di Ingegneria Industriale, Università degli Studi di Salerno, Via Ponte don Melillo, I-84084 Fisciano (SA), Italy*
[2]*Fachbereich Physik, Naturwissenschaftlich-Technische Fakultät, Universität Siegen, 57068 Siegen, Germany*
(Dated: March 31, 2013)

We discuss systems of ions in segmented linear Paul traps for the quantum simulation of spin models which exhibit long-distance entanglement (LDE) in the ground state. The axial potential can be tailored to create different coupling patterns suitable to create LDE. Microwave pulses are used to implement various kinds of spin-spin interaction Hamiltonians, which can be varied adiabatically thereby realizing the adiabatic preparation of the ground states of quantum spin Hamiltonians exhibiting LDE.

arXiv:1304.0261v1 [quant-ph] 31 Mar 2013

I. INTRODUCTION

Entanglement is a central resource for quantum technological applications [1, 2]. Great effort has been devoted to the generation and distribution of entanglement over long distances, with the intent of realizing large-scale protocols of quantum information and communication technologies [3–22].

Particularly intriguing in this context is the prediction that certain spin models are naturally endowed with peculiar entanglement properties in their ground state which could be profitable for quantum communication purposes, for example, between different spatial regions within a quantum processor. Specifically, the concept of long-distance entanglement (LDE) has been introduced and discussed in order to identify the occurrence of sizeable nonlocal quantum correlations between distant, non-directly interacting spins in quantum spin chains and networks [17–22]. This phenomenon emerges in models with non degenerate ground states, when the end spins (spins at the boundary of the system) interact weakly with their immediate neighbors, such that a strongly correlated bulk mediates effective interactions between the distant, non directly interacting, end spins. In this work we discuss the feasibility of schemes for the experimental observation of this effect using trapped ions as quantum simulators of quantum spin models.

Trapped ions are highly versatile systems which have been proven to be extremely effective in quantum technological applications. The simulation of quantum models of strongly interacting quantum matter with trapped ions holds promise for the investigation of those quantum dynamics that remain so far unexplored due their inescapable complexity [23]. Indeed, the natural many-body dynamics of trapped atoms is very rich and interesting by itself; on the other hand, in the present work we will be mainly concerned with the subtle and intriguing task of realizing models that are not directly provided by the natural, i.e. non engineered, physics of trapped ions. Although spin interactions emerge quite naturally in ion chain systems, engineering and control of a desired complex Hamiltonian can be highly challenging tasks with high pay-off. Spectacular proof of principle experimental demonstrations [24–27] have shown the potential of trapped ion based quantum simulators. However, so far none of these experiments has explored the ground state of spin models which are expected to exhibit highly nonclassical properties. Moreover, no experiment so far has faced the simultaneous occurrence of all the following features combined together: 1) sophisticated shaping of the trap potentials in order to suppress the effect of long-range interactions; 2) highly controlled adiabatic processes driving the system to the ground state; 3) full implementation of Trotterization (Trotter expansion) in order to generate the relevant spin-spin interactions in all the needed directions and components.

In the following we will discuss schemes to simulate ground states of complex quantum systems, exhibiting highly nonclassical properties, by the use of trapped ions featuring aspects 1)-3) listed above. Specifically, we will explore the capabilities of trapped ion systems for the quantum simulation of spin models, and we will apply them to propose the first demonstration of LDE in quantum spin chains. LDE is a global nonclassical effect which, on the other hand, can be monitored by the analysis of only two spins, namely the end spins of the chain. It is therefore a sufficiently simple, yet rich phenomenon which is ideal to be demonstrated using an ion trap quantum simulator. Differing from the previous experiments cited above [25–27] in which the spin coherent manipulation is realized with laser fields, here we focus on segmented ion traps in the presence of a magnetic gradient where the engineering of the quantum dynamics is realized by microwave fields.

The paper is organized as follows. In Sec. II we introduce the systems and discuss the basic features of the scheme that we implement for the simulation of long distance entanglement. In Sec. III we discuss how to tailor the spin-spin interactions and we describe the scheme of pulses for the simulation of spin Hamiltonians. In Sec. IV we discuss the results for the adiabatic preparation of the ground state and discuss the experimental feasibility of the protocol. Finally, in Sec. V we draw conclusions and discuss possible outlooks.

*Corresponding author: illuminati@sa.infn.it

II. THE SYSTEM

Doppler cooled ions held in a segmented ion trap [28, 29] and exposed to a magnetic field gradient realize effective spin-1/2 models [30–33]. The effective spin-spin interactions induced by the magnetic field are of Ising type and can be adjusted by tailoring the axial trapping potential. In particular, if the ions are sufficiently cold, such that the ion motion can be neglected (the validity of this approximation is discussed in Sec. IV B), the effective system of N spins is described by the Ising Hamiltonian

$$\overline{H}_{Ising}^{(z)} = \overline{H}_z + H_{zz}$$

$$\overline{H}_z = \frac{\hbar}{2} \sum_{j=1}^{N} \omega_j \sigma_j^z$$

$$H_{zz} = -\frac{\hbar}{2} \sum_{j,k} J_{j,k} \sigma_j^z \sigma_k^z, \qquad (1)$$

where the resonance frequencies of the atomic spins ω_j depend on the external magnetic field $B(x_{0,j})$ at the equilibrium position of the ion $x_{0,j}$ [34]. The spin-spin couplings are in general long range and their magnitude depends on the trapping potential and on the spatial derivative of the spin resonance frequency that, in turn, is determined by the magnetic field gradient. They are given by

$$J_{j,k} = \frac{\hbar}{2} \frac{\partial \omega_j}{\partial x_j}\Big|_{x_{0,j}} \frac{\partial \omega_k}{\partial x_k}\Big|_{x_{0,k}} (A^{-1})_{jk}, \qquad (2)$$

Here, A, whose elements are $A_{j,k} = \frac{\partial^2 V(x_1, \cdots x_N)}{\partial x_j \partial x_k}\Big|_{x_\ell = x_{0,\ell}, \forall \ell}$, is the Hessian matrix of the potential energy function $V(x_1, \cdots x_N)$ that confine the ions with x_j indicating the position of the ion j. Besides, the magnetic gradient allows also for the addressing of individual spins with microwave field which can, therefore, be used to manipulate the spin dynamics.

A. General considerations

Spin Hamiltonians with non-trivial ground state correlations (as in the case of LDE) are in general characterized by non-commuting spin-spin interaction terms. This is not the case of the simple Ising Hamiltonian (1) in which only interactions terms of the form $\sigma_j^z \sigma_k^z$ are present. Therefore, the simulation of LDE requires the ability to engineer interactions along a different axes, described for example by a term of the form $\sigma_j^x \sigma_k^x$. Such an effective interaction can be induced using a sequence of $\pi/2$ microwave pules that realize the transformation $e^{-i\pi\sigma_j^y/4} \sigma_j^z e^{i\pi\sigma_j^y/4} = \sigma_j^x$ over all the spins. In particular, a free evolution sandwiched by two trains of $\pi/2$ pulses (each pulse addresses a particular ion $j = 1, ..., N$) with opposite phase performs the following transformation

$$e^{-i\frac{\pi}{4}\sigma_N^y} \cdots e^{-i\frac{\pi}{4}\sigma_1^y} e^{-i\overline{H}_{Ising}^{(z)}t} e^{i\frac{\pi}{4}\sigma_1^y/4} \cdots e^{i\frac{\pi}{4}\sigma_N^y/4} = e^{-i\overline{H}_{Ising}^{(x)}t}, \qquad (3)$$

and realizes an Ising interaction along the x-axes. In order for this transformation to be effective, the duration of the pulses have to be sufficiently short so that the evolution due to the spin-spin interactions can be neglected. This is achieved with a sufficiently strong microwave driving field resulting in a Rabi frequency $\Omega \gg J_{j,k}$. On the other hand each microwave pulse should operate on a single spin, and its effect on the other spins should be negligible. This imposes a limit on the maximum allowed intensity of the driving field $\Omega \ll \Delta$, where Δ indicates the frequency difference between neighboring spin resonances.

The simultaneous interaction along z and x can be simulated by Trotterization, namely by repeated, fast application of the two kind of interactions [35]. Provided that the interaction time τ/n is sufficiently small, it is possible to approximate

$$e^{-i\left[\overline{H}_{Ising}^{(x)} + \overline{H}_{Ising}^{(z)}\right]\tau} \simeq \left[e^{-i\overline{H}_{Ising}^{(z)}\tau_1/n} e^{-i\overline{H}_{Ising}^{(x)}\tau_2/n}\right]^n, \qquad (4)$$

and to generate a stroboscopic evolution which simulates a Hamiltonian that is the sum of two Ising Hamiltonians with interactions along two orthogonal axes.

We also note that typically the parameters in the Hamiltonian $\overline{H}_{Ising}^{(z)}$ defined in Eq. (1) are such that the spin-spin coupling strengths are much smaller then the single site energy, $J_{j,k} \ll \omega_\ell$, which hence dominate the dynamics of this model. Nevertheless we note that we are interested in the situation in which the system is driven by a series of microwave pulses. In this case, as demonstrated in the next section, the relevant dynamics is that obtained in a reference frame rotating at the driving field frequency. In this representation, the relevant single site energy is in fact given by the detuning $h = \omega_j - \overline{\nu}_j$ between spin resonance frequency and driving field frequency, which can therefore be adjusted and controlled during the dynamics.

These results can eventually be used for the adiabatic preparation of the ground state of, for example, XX Hamiltonians. The system is prepared initially in the ground state of a sufficiently simple Hamiltonian which is easy to prepare: In our case it consists of the ferromagnetic/fully polarized spin state which is the ground state of the Ising Hamiltonian with finite magnetic field ($H_{initial} = \hbar\, h/2 \sum_j \sigma_j^z - \hbar/2 \sum_{j,k} J_{j,k} \sigma_j^z \sigma_k^z$). Then, the effective magnetic field is slowly switched off (h is reduced) while the interaction along x is turned on by tuning the relative duration of the evolutions under the two Hamiltonians $\overline{H}_{Ising}^{(x)}$ and $\overline{H}_{Ising}^{(z)}$. If the variation of the parameters is sufficiently slow, then the system remains in the instantaneous ground state. And eventually it approaches the ground state of the final modified target Hamiltonian $H_{final} = -\hbar/2 \sum_{j,k} J_{j,k} \left(\sigma_j^z \sigma_k^z + \sigma_j^x \sigma_k^x\right)$ where the effective magnetic field is zero and both interactions along x and z are present. This Hamiltonian exhibits ground state long distance entanglement when the end spins are weakly coupled to the bulk [17–22].

However, in general the typical harmonic trapping potential of linear ion traps induces long range interactions with maximum couplings at the end of the chain. Thus, in order to simulate ground state LDE, the trapping potential has to be carefully engineered and the end spins interactions have to be made weak. This can be realized with segmented micro-traps

as discussed in Sec. III A.

III. ENGINEERING OF SPIN HAMILTONIANS WITH TRAPPED IONS

In this section we study how to manipulate the coupling strengths $J_{j,k}$ and how other kinds of spin Hamiltonians can be designed. To be specific, we present detailed calculations for an existing micro-structured ion trap [28, 29]. The principles used to obtain the concrete results presented in what follows are, of course, applicable to other segmented traps as well.

A. Tailoring the coupling constants in a segmented trap

In the following we will discuss how to generate the axial trapping potential which results in the desired coupling pattern. The theory follows [36], where coupling patterns were calculated, when ions are held in a micro-structured trap, which means, that each single ion or ion chain is located at the bottom of an approximately harmonic potential. The separation of potentials is large (on the order $100\,\mu$ m) and the coupling between different sites can become impractically small (Hz) for the purpose described in this article. Here, we consider ions held in common closely separated and anharmonic wells, and we tune both the harmonic and anharmonic part to obtain the desired coupling pattern.

The effective potential can be written as

$$\phi_{\text{eff}} = \frac{P_{\text{rf}}}{P_0}\phi_{\text{rf}} + \sum_i \frac{U_i}{U_0}\phi_i \qquad (5)$$

where ϕ_{rf} is the effective rf potential present at an rf power level $P_{\text{rf}} = P_0$. ϕ_i is the dc potential originating from electrode i set to the voltage $U_i = U_0$. The effect of the rf field on the axial potential is neglected in the following discussion.

The potential ϕ_i of a single segment electrode set to a non vanishing voltage is bound to be symmetric with respect to the center of that electrode for the approximation of harmonic trapping and remains ideally symmetric for periodic boundary conditions. This leads also to symmetric ion configurations, unless the 'history' of the string (e. g. applying intentionally asymmetric potential patterns) was used to split the chain off-centre. We are in a regime, where the electrodes are much wider compared to inter ion separations, so potential or electric field cannot independently be chosen at each ion position.

With a given voltage pattern applied to the electrodes, and an initial guess of ion positions, one can calculate equilibrium positions by minimizing the total energy. Note that several local minima are possible, corresponding to different numbers of ions in wells. In addition, permutations of ion positions yield identical total energies. After the equilibrium ion positions have been determined, we calculate the normal modes of an ion string, the Zeeman shifts of individual ions and the resulting coupling constants. For all numerical simulations presented in the rest of this paper, we assume an axial magnetic field gradient of 50 T/m.

The desired coupling pattern is symmetric (a bulk chain weakly coupled to outer ions) so we consider symmetric potential configurations and ion positions. The symmetry can easily be broken at will, either by applying non-symmetric voltage patterns, or by loading different numbers of ions per site. We create up to three potential wells, and depending on wells up to four basic scenarios can be distinguished.

For small excursion Δx_i of ion i from the equilibrium position, the motion of the chain can be decomposed into normal modes, which is equivalent to say that the force F_{ij} on ion j depends linearly on the excursion pattern $\vec{\Delta x}$ as

$$\vec{F} = \hat{M}\vec{\Delta x}$$

F_{ij} has two contributions:

1. the sum of changes of all Coulomb forces

2. the change due to a different position in the external potential

So $\hat{M}$ can be read such that the column vectors are the forces on ion j if ion i is moved by a unit length from its equilibrium position.

$$M_{ij} = \begin{cases} \dfrac{q^2}{2\pi\epsilon_0}\dfrac{1}{(x_i-x_j)^3} & i \neq j \\ \\ q\,\partial_x^2\phi(x)|_{x=x_i} - \sum_{k>i} M_{ik} & i = j\,. \end{cases}$$

Coupling can thus be interpreted in three steps:

1. a flip of one ion i would lead to a position change in a magnetic gradient. The size of that change depends only on the magnetic moment, the gradient, and the local curvature of the trapping potential

2. the new position changes the equilibrium positions of all other ions. For ion j the size of the change is proportional to the size of the position change of ion i and the local potential curvature at the position of ion j

3. the position change Δx_j is translated to a change of the level splitting $\Delta\omega_j$. This change is proportional to Δx_j and the gradient at the position x_j

In the following, three potential shapes are discussed and values for ion positions, qubit level splittings (for zero offset field), normal modes and couplings are given. Note that, for symmetric potentials and ion positions, the couplings are also symmetric, thus

$$J_{1,2} = J_{3,4} \quad \text{and} \quad J_{2,3} = J_{3,4}$$

1. Coupling in a common well

When one or more segments are set to a negative voltage, and the others are kept at ground, a single trapping zone is created and the potential is predominantly harmonic. The coupling pattern shows strong next neighbor coupling and also

substantial coupling beyond next neighbors. Figure 1 shows the potential in the vicinity of the center of symmetry together with the equilibrium positions and the resulting coupling pattern. Numerical values for positions, levels splittings, normal modes and couplings are given in Tab. I.
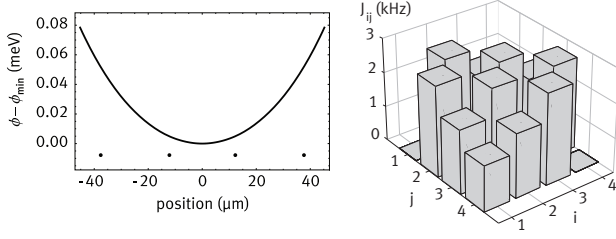

FIG. 1: Axial potential and equilibrium ion positions for a predominantly harmonic single well

i	1	2	3	4
$x_{0,i}$ (μm)	-37.7	-12.2	12.2	37.7
$\omega_i/2\pi$ (MHz)	-26.4	-8.5	8.5	26.4
$\nu_i/2\pi$ (kHz)	36.1	61.6	83.3	101.8

i,j	1,2	1,3	1,4	2,3
J_{ij} (kHz)	2.64	1.85	1.32	2.67

TABLE I: Positions x_i, qubit splittings ω_i, normal modes ν_i and couplings J_{ij} for an ion chain in an approximately harmonic axial trapping potential.

2. Coupling in three wells

Trapping ions in three independent wells allows an intuitive approach to generate LDE: the inner ions are confined in a common well and couple strongly. The outer ions sit in separate wells and thus show only small coupling to the center 'bulk' string (see fig. 2, left image). In fact, separating the outer ions might generate outer wells with a steep confinement, further reducing the coupling to all other ions. This can be seen in the resulting coupling pattern (see fig. 2, right image). Numerical values for positions, levels splittings, normal modes and couplings are given in Tab. II.
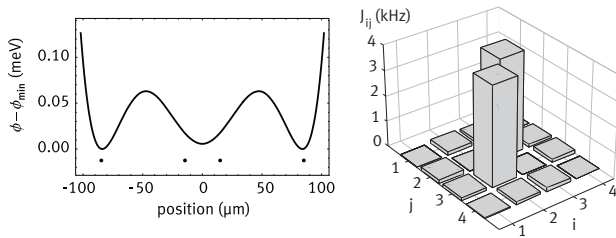

FIG. 2: Axial potential and equilibrium ion positions for ions confined in three wells

i	1	2	3	4
$x_{0,i}$ (μm)	-85.0	-14.9	14.9	85.0
$\omega_i/2\pi$ (MHz)	-59.5	-10.4	10.4	59.5
$\nu_i/2\pi$ (kHz)	36.1	66.6	85.4	85.5

i,j	1,2	1,3	1,4	2,3
J_{ij} (kHz)	0.14	0.10	0.00	3.93

TABLE II: Positions x_i, qubit splittings ω_i, mechanical normal modes ν_i and couplings J_{ij} for an ion chain in three approximately harmonic axial trapping potential.

3. Coupling in a single strongly anharmonic well

Making a well strongly anharmonic, substantially alters the normal mode spectrum and allows to generate a pattern suitable for creating LDE. Changing the softness of the outer wells allows to choose the ratio of the coupling of outer ions to their neighbors with respect to the coupling between the two center ions in a wide range (see fig. 3). Note that this potential configuration differs only slightly from the situation shown before. This indicates a strong dependence of the coupling on the applied voltages and puts strict requirements on voltage stability and accuracy which have to be taken account the the design of the voltage supplies[37]. Numerical values vor positions, levels splittings, normal modes and couplings are given in Tab. III.
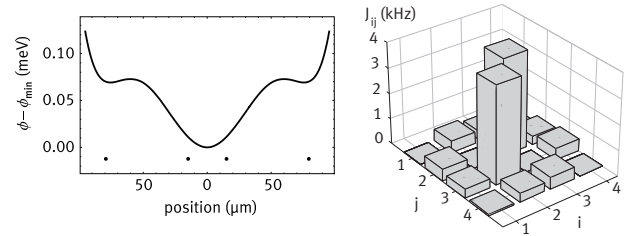

FIG. 3: Axial potential and equilibrium ion positions for ions confined in a single anharmonic well, whose shape generates a coupling pattern suitable for creating LDE. The coupling of the inner ions compared to the coupling to the end ions can be scaled by choosing the anharmonicity.

i	1	2	3	4
$x_{0,i}$ (μm)	-79.5	-15.1	15.1	79.5
$\omega_i/2\pi$ (MHz)	-55.6	-10.5	10.5	55.6
$\nu_i/2\pi$ (kHz)	36.1	52.9	53.0	65.9

i,j	1,2	1,3	1,4	2,3
J_{ij} (kHz)	0.14	0.10	0.00	3.93

TABLE III: Positions x_i, qubit splittings ω_i, normal modes ν_i and couplings J_{ij} for an ion chain in a strongly anharmonic axial trapping potential.

4. A Suitable Potential to Simulate LDE

A pattern similar to the previous section is used for the simulations in the rest of the article. Compared to Sec. III A 3, all voltages are scaled up by a factor of four, resulting in approximately two times stiffer axial trapping frequencies which makes trapping more robust and reduces the populations in higher vibrational modes. The couplings on the other hand are reduced by a factor of 4, slowing down the speed of the simulation and thus requiring longer coherence. The long range interactions are small, and the end spins are weakly coupled giving appropriate starting conditions to generate LDE. Numerical values for positions, levels splittings, normal modes and couplings are given in Tab. IV.

i	1	2	3	4
$x_{0,i}$ (μm)	-76.8	-9.6	9.6	76.8
$\omega_i/2\pi$ (MHz)	-53.7	-6.7	6.7	53.7
$\nu_i/2\pi$ (kHz)	71.3	88.3	88.3	129.6

i, j	1,2	1,3	1,4	2,3
J_{ij} (kHz)	0.04	0.03	0.00	0.99

TABLE IV: Positions x_i, qubit splittings ω_i, normal modes ν_i and couplings J_{ij} for an ion chain in three approximately harmonic axial trapping potential.

B. Spin dynamics with microwave pulses

The spin dynamics can be manipulated using external microwave fields which can drive selectively a given spin by tuning the driving frequency to the corresponding resonance. The hamiltonian for the interaction between the ion spins and the driving field in the rotating wave approximation and neglecting the ion motion (see Sec. IV B for an analysis of the effects of the motion) takes the form

$$\overline{H}_L(t) = -i\hbar\Omega(t) \sum_j \left\{ \sigma_j^+ e^{-i[\overline{\nu}(t)t+\varphi(t)]} - \sigma_j^- e^{i[\overline{\nu}(t)t+\varphi(t)]} \right\}. \quad (6)$$

In general the amplitude Ω, the frequency $\overline{\nu}$, and the phase φ of the driving field can be time dependent. In particular we consider a sequence of step-like driving pulses: We identify a set of time instants t_m with $m = 0, 1, 2, \cdots$ which define a corresponding set of time intervals $(t_{m-1}, t_m]$ during which the driving Hamiltonian is constant, ($\Omega(t) = \Omega_m$, $\overline{\nu}(t) = \overline{\nu}_m$ and $\varphi(t) = \varphi_m$ for $t \in (t_{m-1}, t_m]$). In certain intervals the driving field can also be zero. If we define the square-pulse function

$$\epsilon_m(t) = \theta(t - t_{m-1}) - \theta(t - t_m) \quad (7)$$

with $\theta(t) = 0$ for $t < 0$ and $\theta(t) = 1$ for $t \geq 0$, then Eq. (6) takes the form

$$\overline{H}_L(t) = \sum_m \epsilon_m(t)\overline{H}_L^{(m)}(t) \quad (8)$$

where

$$\overline{H}_L^{(m)}(t) = -i\hbar\Omega_m \sum_j \left[\sigma_j^+ e^{-i(\overline{\nu}_m t+\varphi_m)} - h.c. \right]. \quad (9)$$

In each time interval in which $\Omega_m \neq 0$, the driving frequency is close to resonance to a single spin j_m, with a small detuning h_m, that is $\overline{\nu}_m = \omega_{j_m} - h_m$.

The spin dynamics can be further harnessed by controlling the external magnetic field. Here we are interested in situations in which the spin-spin couplings $J_{j,k}$ are fixed. In particular $J_{j,k}$ does not change when, for example, the direction of the B field is inverted. On the other hand in this case the spin resonances are affected. Specifically, the difference between the spin resonance frequency

$$\Delta_{j,k} = \omega_j - \omega_k$$

changes in sign when the direction of the magnetic field is inverted. Hence in each step the spin frequency can be defined as

$$\omega_j^{(m)} = \omega_0 + \eta_m\omega_{0j},$$

where ω_0 is an offset frequency, ω_{0j} the frequency relative to the offset and $\eta_m = \pm 1$ accounts for two possible direction of the magnetic field.

The system Hamiltonian is

$$\overline{H}(t) = \sum_m \epsilon_m(t)\left[\overline{H}_z^{(m)} + H_{zz} + \overline{H}_L^{(m)}(t)\right]. \quad (10)$$

where $\overline{H}_z^{(m)} = \frac{\hbar}{2} \sum_{j=1}^N \omega_j^{(m)}\sigma_j^z$.

The time dependence of the driving Hamiltonian $\overline{H}_L^{(m)}(t)$ can be removed in a reference frame rotating at the driving field frequency as discussed in App. A. The dynamics in the two representations are related by a unitary and local transformation, thus the corresponding entanglement properties are equal.

The system Hamiltonian in the new representation takes the form (see App. A)

$$H(t) = \sum_{m \,:\, \Omega_m=0} \epsilon_m(t)\left[H_{z,0}^{(m)} + H_{zz}\right]$$
$$+ \sum_{m \,:\, \Omega_m\neq0} \epsilon_m(t)\left[H_{z,1}^{(m)} + H_{zz} + H_L^{(m)}\right] \quad (11)$$

with

$$H_{z,0}^{(m)} = \frac{\hbar}{2}h_m \sum_{j=1}^N \sigma_j^z$$

$$H_{z,1}^{(m)} = \frac{\hbar}{2} \sum_{j\neq j_m} \left[\eta_m \Delta_{j,j_m} + h_m\right]\sigma_j^z$$

$$H_L^{(m)} = -i\hbar\Omega_m \sum_j \left\{ \sigma_j^+ e^{-i[\phi_j^{(m)}-\phi_{j_m}^{(m)}]} - h.c. \right\}. \quad (12)$$

Here the sum over the time intervals is divided into two sums over the intervals in which the driving field is on and off respectively, and the label j_m indicates the spin which is driven

quasi resonantly in each time interval. Moreover we have set the driving phase φ_m to the value $\varphi_m = -\phi_{j_m}^{(m)}$ with

$$\phi_j^{(m)} = \sum_{m'=1}^{m-1} \left[\nu_j^{(m'+1)} - \nu_j^{(m')} \right] t_{m'}, \qquad (13)$$

where

$$
\begin{aligned}
\nu_j^{(m)} &= \eta_m \omega_j - h_m & \text{when } \Omega_m = 0 \\
\nu_j^{(m)} &= \eta_m \omega_{j_m} - h_m & \text{when } \Omega_m \neq 0.
\end{aligned} \qquad (14)
$$

So, in this representation, the spin j_m sees an effective magnetic field along the y-axes.

C. Stroboscopic engineering of the *XX* spin dynamics

In order to engineer the dynamics of an *XX* quantum spin model we consider a sequence of driving pulses made of $2N + 2$ steps ($m = 1, \cdots 2N + 2$) and identified by the corresponding values of the driven spin j_m, the direction of the magnetic field η_m, the laser intensity Ω_m and the duration of the time step $t_m - t_{m-1}$. During the all sequence the value of the detunings is fixed $h_m = h$. The sequence is made as follows: after a free evolution (no driving: $m = 1$ and $\Omega_1 = 0$), of time $t_1 - t_0 = \Delta t_1$, each spin is driven sequentially from the last to the first (such that for $m = 2, \cdots N + 1$, $\left\{ j_m = N - m + 2, \eta_m = -1, \Omega_m = -\overline{\Omega}_{j_m}, t_m - t_{m-1} = \delta t_{j_m} \right\}$, where the actual values of $\overline{\Omega}_{j_m}$ and δt_{j_m} are identified below); then after another free evolution (no driving: $m = N + 2$ and $\Omega_{N+2} = 0$), of time $t_{N+2} - t_{N+1} = \Delta t_2$, the spins are driven sequentially from the first to the last (such that for $m = N + 3, \cdots 2N + 2$, $\left\{ j_m = m - N - 2, \eta_m = 1, \Omega_m = \overline{\Omega}_{j_m}, t_m - t_{m-1} = \delta t_{j_m} \right\}$). Note that in the first train of pulses the values of η_m and Ω_m are the opposite of that in the second train of pulses. This is realized changing the direction of the magnetic field, that realizes the transformation $\eta_m \to -\eta_m$, and adding a phase of π to the driving field, that realizes the transformation $\Omega_m \to -\Omega_m$.

As discussed in App. B the evolution operator at the final time $\bar{t} = t_{2N+2} = \Delta t_1 + \Delta t_2 + \sum_j \delta t_j$, corresponding to this sequence, with the parameters in each time interval which satisfy the relations

$$
\begin{aligned}
\overline{\Omega}_{j_m} \delta_{j_m} &= \frac{\pi}{4} \\
\frac{1}{2} \sum_{j > j_m} \Delta_{j,j_m} \delta t_j &= n_{j_m} \pi \quad \text{with } n_{j_m} \in \mathbb{Z},
\end{aligned} \qquad (15)
$$

can be approximated, in the limit $\left| \Delta_{j,j_m} \right| \gg |\Omega_m| \gg |h_m|, |J_{j,k}|$, as

$$U_{\bar{t}} = e^{-iH_{Ising}^{(x)} \Delta t_2} \, e^{-iH_{Ising}^{(z)} \Delta t_1} \qquad (16)$$

where

$$H_{Ising}^{(\zeta)} = \frac{h}{2} \sum_{j=1}^{N} \sigma_j^\zeta - \frac{1}{2} \sum_{j,k} J_{j,k} \sigma_j^\zeta \sigma_k^\zeta, \quad \text{for } \zeta \in \{x, z\} \ (17)$$
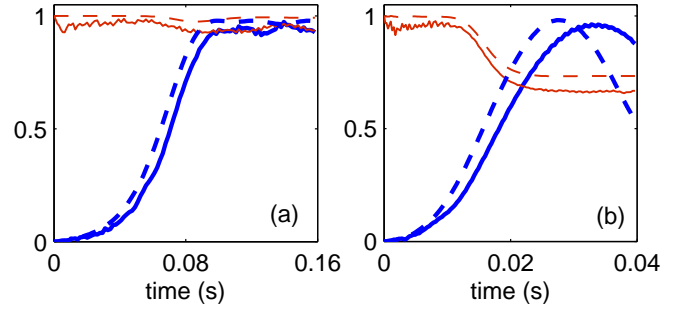

FIG. 4: End-to-end concurrence (thick, blue lines) and fidelity (thin, red lines) with the instantaneous ground state for a four ion system. The dashed line are obtained integrating the time dependent effective Hamiltonian in Eq. (22) with the time dependence defined in Eq. (23) ($h_0 = 2\pi \times 0.99 kHz$); The solid lines are obtained using the Hamiltonian in Eq. (11), following the pulse scheme described in Sec. III C and with the stepwise variation of the parameters h and α. The spin-spin coupling constant and the spin resonance frequencies are identified in Sec. III A 4. Plots (a) and (b) differ for the velocity of the adiabatic manipulation: in (a) $r = 2\pi \times 10 Hz$ in (b) $r = 2\pi \times 40 Hz$. The other parameters are: (a) $\Delta t_1 = 64 \mu s$ and $\{\delta_1, \cdots \delta t_4\} = \{1.87, 1.95, 1.94, 1.87\} \mu s$, and (b) $\Delta t_1 = 80 \mu s$ and $\{\delta_1, \cdots \delta t_4\} = \{1.57, 1.61, 1.61, 1.57\} \mu s$

The stroboscopic evolution at times $n\bar{t}$, with $n \in \mathbb{N}$, given by the repeated application of this sequence of pulses is described by the operator

$$U_{n\bar{t}} = U_{\bar{t}}^n = \left(e^{-iH_{Ising}^{(x)} \Delta t_2} e^{-iH_{Ising}^{(z)} \Delta t_1} \right)^n. \qquad (18)$$

According to the Trotter formula [..cite]

$$e^{-i(H_1 + H_2)t} = \lim_{n \to \infty} \left(e^{-iH_1 t/n} e^{-iH_2 t/n} \right)^n, \qquad (19)$$

and in the limit $\Delta t_1, \Delta t_2 \ll \left| J_{j,k} \right|^{-1}, |h|^{-1}$, we can approximate

$$U_{n\bar{t}} \simeq e^{-i\left(H_{Ising}^{(z)} + \alpha H_{Ising}^{(x)} \right) n\Delta t_1} = e^{-i\beta \left(H_{Ising}^{(z)} + \alpha H_{Ising}^{(x)} \right) n\bar{t}} \qquad (20)$$

where

$$
\begin{aligned}
\alpha &= \frac{\Delta t_2}{\Delta t_1} \\
\beta &= \frac{\Delta t_1}{\bar{t}} = \frac{\Delta t_1}{(1 + \alpha)\Delta t_1 + 2 \sum_j \delta t_j}.
\end{aligned} \qquad (21)
$$

This result demonstrates that the stroboscopic evolution described above approximate the evolution, at times $n\bar{t}$, of a spin system with the effective Hamiltonian

$$H_{\text{eff}} = \beta \left[H_{Ising}^{(z)} + \alpha H_{Ising}^{(x)} \right]. \qquad (22)$$

IV. ADIABATIC PREPARATION AND STROBOSCOPIC/PULSED DYNAMICS

The parameters h, α and β can be varied adiabatically in order to prepare the ground state of an *XX* hamiltonian as discussed in App. C.The effective external magnetic field h can
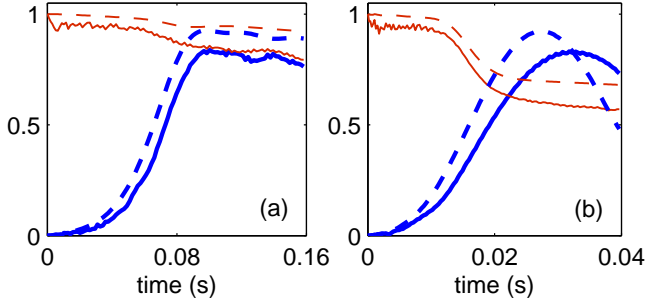
FIG. 5: As in Fig. 4 with a dephasing rate (a) $\gamma = 2\pi \times 0.1 Hz$ and (b) $\gamma = 2\pi \times 0.4 Hz$.

be varied by adjusting the detuning between the driving field and the ion-spin resonance frequencies. On the other hand α, and correspondingly β are varied by controlling the time Δt_2.

The system is initialized in the ferromagnetic state with all the spins aligned along the z-axes that is the ground state of the Ising Hamiltonian ($\alpha = 0$). The value of h is initially set to some value h_0 in order to remove the ground state degeneracy.

The parameters α and h are then slowly varied to realize the adiabatic preparation of the LDE. In particular during each sequence of pulses, that is described in Sec.III C, the values of h and α are kept fixed, while they are varied from sequence to sequence in order to realize a stepwise approximation of the functions (see App. C)

$$
\begin{aligned}
\alpha(t) &= 1 - e^{-rt} \\
h(t) &= h_0 e^{-rt}.
\end{aligned}
\tag{23}
$$

The efficiency of this stepwise adiabatic protocol is analyzed numerically by evaluating the evolution corresponding to the Hamiltonian (11) with the time sequence and the parameters discussed in Sec. III C, and the corresponding stepwise variation of h and α. The results are shown in Figs. 4 and 5 (solid lines) for different values of the rate of variation r. They are compared with that obtained by the numerical integration of the Shrödinger equation with the effective time dependent Hamiltonian 22 where the time dependent parameters α and h are defined in Eq. (23) (dashed lines).

In both cases the protocol is characterized in terms of the fidelity between the resulting state and the expected instantaneous ground state of the effective Hamiltonian (22) (red, thin curves), and in terms of the end-to-end concurrence (blue, thick curves). The fidelity indicates how far is the resulting state from the expected one: Fidelity equal to one corresponds to perfect adiabatic following; while equal fidelity for both the standard adiabatic evolution (dashed lines) and the step-wise adiabatic evolution (solid lines) means that the protocol realizes a perfect simulation of the effective Hamiltonian. On the other end, the concurrence measure the entanglement between the end spins, and concurrence equal to one indicates a maximally entangled Bell state.

When r is sufficiently small (Fig. 4) (a) the ground state preparation is quite good: The fidelity is close to one and as expected the ground state exhibits large entanglement. When

on the other and the rate is too large (Fig. 4) (b) then the evolution is no more adiabatic and the system ends up in a state which is not the ground state of the final hamiltonian and the fidelity is reduced. Nevertheless also in this case, the end-to-end entanglement can be very large at certain times meaning that the end spins approach a Bell state. Also in this case the bulk efficiently mediates an interaction between the end spins which entangle them efficiently.

In all cases the evolution performed with the effective Hamiltonian and that obtained via the sequence of pulses are very similar meaning that the protocol is faithful. The efficiency of the second is only slightly reduced but the overall behaviors are consistent.

A. Effect of spin dephasing

Fig. 5 is evaluated including the dephasing of the spins. It is obtained by solving a master equation for the spins dynamics of the form

$$
\dot\rho = -i\left[H(t),\rho\right] + \mathcal{L}_D\rho
\tag{24}
$$

where $H(t)$ corresponds to the Hamiltonian (11) for the solid lines and to the effective Hamiltonian (22) for the dashed lines. Moreover $\mathcal{L}_D$ accounts for the spins dephasing at rate γ and takes the form

$$
\mathcal{L}_D\rho = \frac{\gamma}{2}\sum_j \left(\sigma^z_j\,\rho\,\sigma^z_j - \rho\right).
\tag{25}
$$

As expected, the dephasing reduces the efficiency of the scheme. In Fig. 5 (b) the entanglement of the end spins is still relatively high with a dephasing time of $\sim 0.4s$. The scheme is expected to be resistant to stronger dephasing (smaller dephasing time) when the coupling constants $J_{j,k}$ are larger. This could be obtained with a stronger gradient of the external magnetic field.

B. Mechanical effects

So far we have neglected the motion of the ions. Internal electronic dynamics and motion can be coupled by an electromagnetic filed. In particular when the ions are in a magnetic gradient also long wavelength radiation, as microwaves, can have a significant mechanical effect allowing for example for sideband cooling [30, 31, 39]. In the following we justify our treatment in which we neglect the atomic motion.

In a magnetic gradient the coupling between an ion j and a mechanical normal mode k is scaled by the effective Lamb-Dicke (LD) parameters [31]

$$
\eta_{j,k} = \sqrt{\frac{\hbar}{2m\,\overline\omega_k}}\,\frac{\mu_B\,g}{\hbar\,\overline\omega_k}\,\frac{\partial B}{\partial x}\bigg|_{x=x_{0,j}} S_{j,k}
\tag{26}
$$

where $\overline\omega_k$ is the frequency of the normal modes, and S is the matrix that diagonalize the Hessian matrix A (see Sec.II) of the potential energy function that confine the ions, that is

$\left(S^T A S\right)_{j,k} = \delta_{j,k}\, m\, \overline{\omega}_j^2$. These parameters are typically small and allow for a systematic expansion of the corresponding dynamics in power of $\eta_{j,k}$. Including the lowest order mechanical effects the Hamiltonian for the interaction between the ions and the driving field (see also Eq. (6)) takes the form

$$\overline{H}_L(t) = -\mathrm{i}\hbar\Omega(t) \tag{27}$$
$$\times \sum_j \left\{ \sigma_j^+ \left[1 + \sum_k \eta_{j,k}\left(a_k^\dagger - a_k\right) \right] \mathrm{e}^{-\mathrm{i}[\overline{\nu}(t)t + \varphi(t)]} - h.c. \right\}$$

where $h.c.$ stands for the hermitian conjugate, and $a_k^\dagger$, a_k are the creation and annihilation operators for the vibrational mode k. This Hamiltonian accounts for sideband transitions at frequencies $\omega_j \pm \overline{\omega}_k$. In order for our analysis to be justified the corresponding excitation probability have to be very small. It can be estimated as

$$\left| \frac{\Omega(t)\, \eta_{j,k}}{\overline{\nu}(t) - \omega_j \pm \overline{\omega}_k} \right|^2 (\overline{n}_k + 1) \ll 1 \tag{28}$$

where $\overline{n}_k$ indicates the average number of motional excitations in the mode k. For the parameters used in Figs. 4 and 5, the largest LD parameter has a value of $\eta_{j,k}^{(max)} \sim 0.14$ and the lowest vibrational frequency is $\overline{\omega}_k^{(min)} \sim 71$ kHz. On the other hand $\Omega = \pi/(4\delta t_j) \sim 70 - 80$ kHz and $\overline{\nu}(t) - \omega_j$ is in the interval $[0, h_0]$, with $h_0 \sim 0.99$ KHz, for the spins which are driven close to resonance, and in the range $[0.07, 0.126]$ GHz for the other spins. The corresponding largest sideband transition probability is $\sim 0.027\,(\overline{n}_k + 1)$, which demonstrate the validity of our results also for Doppler cooled trapped ions, without additional sub Doppler cooling to the ground state of the axial potential. Increasing the gradient of the B field, the coupling strengths increases allowing for a faster preparation; However the system approaches the regime in which the mechanical effects are relevant. In fact, stronger gradient of the magnetic field correspond to larger LD parameters. In turns it imply that the LD expansion up to the first sidebands is no more valid and higher order sideband transition may become relevant hence invalidating our treatment.

C.   Experimental Feasibility

Here, we first consider how a fluctuating coupling constant (due to, for instance, fluctuating electrode voltages) would influence the generation of LDE. Then we briefly outline typical experimental parameters, as are used in the experimental set-up described in [29].

1.   Stability estimates

Let us consider a spin model with Hamiltonian $H = \sum_{j,k} \widetilde{J}_{j,k}\left(\sigma_j^x \sigma_k^x + \sigma_j^z \sigma_k^z\right)$. If the coupling matrix $\widetilde{J} = J$ where J is the one defined in Sec. III A 4, then the ground state end-to-end concurrence is 0.98.
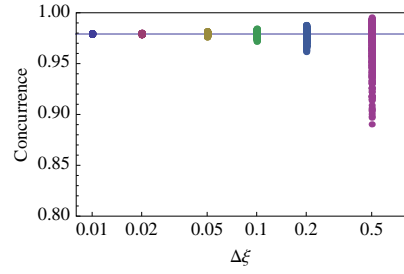

FIG. 6: End-to-end concurrence for random couplings: for each value of the interval of variation $\Delta\xi$ of the random variables $\xi_{j,k}$ the plot shows the concurrence corresponding to 500 different realizations (the 500 points form a vertical segment for each value of $\Delta\xi$). The horizontal line indicates the value 0.92, that is the value of the concurrence for the coupling matrix defined in Sec. III A 4.

Let us now define the random couplings $\widetilde{J}_{j,k} = J_{j,k}\left(1 + \xi_{j,k}\right)$ with $\xi_{j,k}$ uniformly distributed random variables in the range $[-\Delta\xi, \Delta\xi]$. The resulting concurrence are reported in Fig. 6. These results shows that the end-to-end entanglement is sufficiently stable under variations of the spin-spin couplings.

In [29] the operation of a segmented trap with a built-in switchable gradient based on micro-structured solenoid is reported. Different isotopes of Ytterbium with or without hyperfine structure can be trapped. For the experiment proposed here, we use ^{171}Yb with a nuclear spin of $I = 1/2$ yielding two hyperfine levels with $F = 0, F = 1$ in the electronic ground state [33, 43]. Different qubit implementations are possible and magnetic sensitive states can be included to allow for **ma**gnetic **g**radient **i**nduced **c**oupling (MAGIC) [30–32] as required for the experiments discussed here or avoided to yield a quantum memory with a long coherence time. The qubit is manipulated using microwave fields (applied through a conventional wave guide) and Rabi frequencies near $\Omega \approx 100$ kHz on the σ transition and a bare coherence time of the magnetic field sensitive hyperfine qubit on the order of 5 ms have been observed. Applying spin echo techniques [40], dynamical decoupling [41] or dressed states [42], we expect to be able to observe a coherent time evolution on a second timescale. Splitting and merging of ion strings (which involves the generation of anharmonic trapping potentials), as well as shuttling have been demonstrated. Stable trapping could be observed down to axial trap frequencies around $\nu_1 = 2\pi \cdot 40$ kHz.

FIG. 7: Chain of 33 ^{171}Yb ions in our segmented trap.

V.   CONCLUSION AND OUTLOOK

In this theoretical article we have introduced and investigated schemes for the quantum simulation of LDE with trapped ions. In particular, we have shown how to tailor the

trapping potential in order to engineer a specific spin-spin coupling pattern in one-dimensional lattices, and we have designed a sequence of microwave pulses able to engineer effective spin-1/2 Hamiltonians of the gapless and isotropic *XX* type. Finally, we have analyzed the efficiency of the adiabatic quantum preparation of the ground state of an effective Hamiltonian which exhibits LDE, demonstrating its feasibility within the limits of current ion trap technology. In the course of the investigation, we have introduced and combined for the first time trap shaping, adiabatic preparation, and Trotterization of the interactions, three key elements that have never being combined together and that we have proven necessary for the realization, so far not yet attained, of truly and highly nonclassical features of complex models of interacting quantum many-body systems.

We expect to be able to carry out the experiment in a medium-term time scale as detailed in IV C. To improve the level of control over the anharmonicity of the axial trapping potential, it might be necessary to use smaller axial trapping segments, possibly in a surface trap. Larger gradients would boost the coupling and allow for stiffer axial confinement, making the scheme more robust against thermal excitation and external stray fields.

Appendix A: The dynamics in a new reference frame

Let us consider the model described by the Hamiltonian in Eq. (10), and study the dynamics in a new reference frame defined by the unitary transformation

$$U_0(t) = \sum_m \epsilon_m(t) e^{-iH_0^{(m)}(t-t_{m-1})} e^{-iH_0^{(m-1)}(t_{m-1}-t_{m-2})} \cdots e^{-iH_0^{(1)}(t_1-t_0)} + \theta(t_0 - t) \quad (A1)$$

with

$$H_0^{(m)} = \frac{1}{2} \sum_j \nu_j^{(m)} \sigma_j^z \quad (A2)$$

where the actual values of $\nu_j^{(m)}$ are identified below. Since the unitary transformation is local, the entanglement properties in the new representation are the same as that in the original one.

If $|\overline{\psi}(t)\rangle$ is the state in the original representation, then the dynamics of the transformed state $|\psi(t)\rangle = U_0^\dagger(t)|\overline{\psi}(t)\rangle$ is ruled by the Hamiltonian

$$H(t) = U_0^\dagger(t)\overline{H}(t)U_0(t) - \sum_m \epsilon_m(t)H_0^{(m)}$$
$$= \sum_m \epsilon_m(t)\left[H_z^{(m)} + H_{zz} + H_L^{(m)}\right] \quad (A3)$$

with

$$H_z^{(m)} = \overline{H}_z^{(m)} - H_0^{(m)} = \frac{1}{2}\sum_j(\omega_j^{(m)} - \nu_j^{(m)})\sigma_j^z$$

$$H_L^{(m)} = -i\Omega_m \sum_j \left\{\sigma_j^+ e^{-i\left[(\overline{\nu}_m - \nu_j^{(m)})t + \phi_j^{(m)} + \varphi_m\right]} - h.c.\right\} \quad (A4)$$

where

$$\phi_j^{(m)} = \sum_{m'=1}^{m-1}\left[\nu_j^{(m'+1)} - \nu_j^{(m')}\right]t_{m'}. \quad (A5)$$

The last Hamiltonian is obtained exploiting the relation $e^{i\zeta\sigma_j^z t}\sigma_j^+ e^{-i\zeta\sigma_j^z t} = \sigma_j^+ e^{2i\zeta t}$. The values of $\nu_j^{(m)}$ are chosen so that the new Hamiltonian is time independent:

$$\nu_j^{(m)} = \omega_j^{(m)} - h_m \quad \text{when } \Omega_m = 0$$
$$\nu_j^{(m)} = \omega_{j_m}^{(m)} - h_m \quad \text{when } \Omega_m \neq 0. \quad (A6)$$

Moreover the phase is fixed to the value

$$\varphi_m = -\phi_{j_m}^{(m)} \quad (A7)$$

so that the phase of the driving pulse, $\phi_j^{(m)} + \varphi_m$, is zero for the spin j_m which is the one that is close to resonance with the driving field in each time interval m. Thereby we obtain Eq. (11).

The corresponding evolution operator decomposes into the product of evolution operators each one describing the evolution in a single time interval $[t_{m-1}, t_m]$:

$$U(t) = \sum_m \epsilon_m(t)e^{-iH^{(m)}(t-t_{m-1})}e^{-iH^{(m-1)}(t_{m-1}-t_{m-2})}\cdots e^{-iH^{(1)}(t_1-t_0)}, \quad (A8)$$

where

$$H^{(m)} = H_z^{(m)} + H_{zz} + H_L^{(m)}. \quad (A9)$$

Appendix B: The sequence of driving pulses

We are interested in the limit in which $\left|\omega_j - \omega_{j_m}\right| \gg |\Omega_m| \gg |h_m|, |J_{j,k}|$, for $j \neq j_m$. Hence we can approximate the Hamiltonian (11) by retaining only the resonant terms as

$$H(t) \simeq \sum_{m\,:\,\Omega_m=0}\epsilon_m(t)\left[H_{z,0}^{(m)} + H_{zz}\right]$$
$$+ \sum_{m\,:\,\Omega_m\neq0}\epsilon_m(t)\left[H_{z,1}^{(m)} + H_L^{(m)}\right]$$
$$H_{z,1}^{(m)} \simeq \frac{\hbar}{2}\sum_{j\neq j_m}\eta_m\Delta_{j,j_m}\sigma_j^z$$
$$H_L^{(m)} \simeq \hbar\Omega_m\sigma_{j_m}^y. \quad (B1)$$

The evolution operator corresponding to the sequence of pulses described in Sec. III C can be written, using the approximate Hamiltonian (B1), in the form

$$U_{\bar{t}} = e^{-iH_N^{(+)}\delta t_N} \cdots e^{-iH_1^{(+)}\delta t_1} e^{-iH_{Ising}^{(z)}\Delta t_2} e^{-iH_1^{(-)}\delta t_1} \cdots e^{-iH_N^{(-)}\delta t_N}$$
$$\times e^{-iH_{Ising}^{(z)}\Delta t_1} \tag{B2}$$

where

$$H_{Ising}^{(z)} = \frac{h}{2}\sum_{j=1}^{N}\sigma_j^z - \frac{1}{2}\sum_{j,k}J_{j,k}\sigma_j^z\sigma_k^z$$

$$H_{j_m}^{(\pm)} = \pm\left(\overline{\Omega}_{j_m}\sigma_{j_m}^y + \frac{1}{2}\sum_{j\neq j_m}\Delta_{j,j_m}\sigma_j^z\right), \tag{B3}$$

and the total time of the sequence is

$$\bar{t} = \Delta t_1 + \Delta t_2 + \sum_j \delta t_j. \tag{B4}$$

The operator $U_{\bar{t}}$ can be rewritten as

$$U_{\bar{t}} = T_N \cdots T_1\, e^{iH_{Ising}^{(z)}\Delta t_2}\, T_1^\dagger \ldots T_N^\dagger\, e^{-iH_{Ising}^{(z)}\Delta t_1} \tag{B5}$$

where

$$T_{j_m} = e^{-i\mathcal{D}_{j_m}\sigma_{j_m}^z}e^{-i\check{\Omega}_{j_m}\sigma_{j_m}^y\delta t_{j_m}} \tag{B6}$$

with

$$\mathcal{D}_{j_m} = \frac{1}{2}\sum_{j>j_m}\Delta_{j,j_m}\delta t_j \tag{B7}$$

Now we use the relation

$$\Xi(\Gamma,\Delta) \equiv e^{-i\Delta\sigma_j^z}e^{-i\Gamma\sigma_j^y}\sigma_j^z e^{i\Gamma\sigma_j^y}e^{i\Delta\sigma_j^z} = \tag{B8}$$
$$= \cos(2\Gamma)\sigma_j^z + \sin(2\Gamma)\left[\cos(2\Delta)\sigma_j^x + \sin(2\Delta)\sigma_j^y\right],$$

which reduces to $\Xi(\Gamma,\Delta) = \sigma_j^x$ when $\Gamma = \frac{\pi}{4} + n\pi$ and $\Delta = n'\pi$, or when $\Gamma = -\frac{\pi}{4} + n\pi$ and $\Delta = \pm\frac{\pi}{2} + n'\pi$ with $n, n' \in \mathbb{Z}$. Thus setting, for example,

$$\overline{\Omega}_{j_m}\delta_{j_m} = \frac{\pi}{4}$$
$$\mathcal{D}_{j_m} = n_{j_m}\pi \tag{B9}$$

with $n_{j_m} \in \mathbb{Z}$, $\forall j_m$, then

$$U_{\bar{t}} = e^{-iH_{Ising}^{(x)}\Delta t_2}\, e^{-iH_{Ising}^{(z)}\Delta t_1} \tag{B10}$$

where

$$H_{Ising}^{(x)} = \frac{h}{2}\sum_{j=1}^{N}\sigma_j^x - \frac{1}{2}\sum_{j,k}J_{j,k}\sigma_j^x\sigma_k^x. \tag{B11}$$
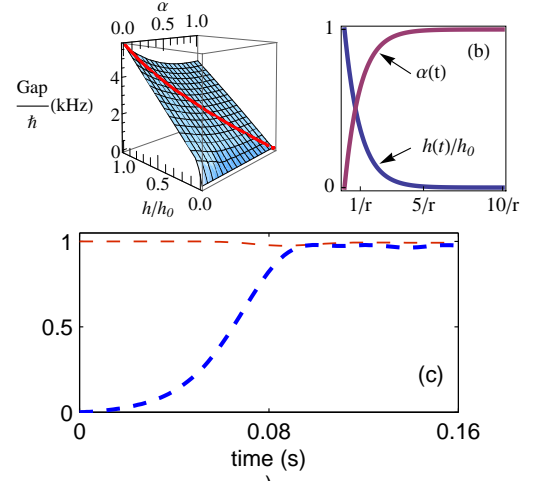

FIG. 8: (a) Gap between ground a first excited state of H_{eff} in Eq. (22) with four ions, in the space of parameters $\{h, \alpha\}$. The red line indicates the gap corresponding to the adiabatic variation of α and h. (b) time evolution of the parameters $\alpha(t)$ and $h(t)$. (c) End-to-end concurrence (thick, blue line) and fidelity with the instantaneous ground state (thin, red line), obtained integrating the time dependent Shrödinger equation with the effective Hamiltonian in Eq. (22) with four ions, and with $h_0 = 2\pi \times 0.99kHz$ and $r = 2\pi \times 10Hz$. The spin-spin couplings are defined in Sec. III A 4. Although not relevant for the present result, in order to be consistent with the results of Sec. IV, we have set the parameter β to the values defined in Eq. (21) (a different value of β corresponds to a rescaling of the energy and correspondingly of the duration of the protocol).

Appendix C: Adiabatic preparation of the Ground state

A system initially in an eigenstate $|\psi_j(0)\rangle$ of its Hamiltonian, follows the instantaneous eigenstate $|\psi_j(t)\rangle$, which derive from the initial state by continuity, when the corresponding Hamiltonian is deformed adiabatically [44]. Condition for the adiabatic evolution is that during the evolution the probability for the transition form the eigenstate $|\psi_j(t)\rangle$ to a different one $|\psi_k(t)\rangle$ ($\forall k$) is negligible, this can be estimated as [44]

$$\sum_{k\neq j}\left|\hbar\frac{\langle\psi_k(t)|\partial H(t)/\partial t|\psi_j(t)\rangle}{\left[E_k(t) - E_j(t)\right]^2}\right|^2 \ll 1. \tag{C1}$$

It means that larger is the difference in energy between the eigenstate state $|\psi_j(t)\rangle$ and all the other, more easily the adiabatic condition can be satisfied.

In particular if initially the system is prepared in the ground state then it will remain in the instantaneous ground state under a slow variation of some Hamiltonian parameters. This idea can be applied to prepare the ground state of complicated Hamiltonians: One can first prepare the ground state of a sufficiently simple one which is easy to prepare. Then the Hamiltonian is adiabatically changed until approaching the final target Hamiltonian. Correspondingly the system will end up in the ground state of the final Hamiltonian.

In our case according to the result of Sec. III C, we are able to generate the dynamics corresponding to the Hamiltonian

(see Eq. (22))

$$H_{\text{eff}}(\alpha, h) = \beta(t) \sum_j h(t) \left[\sigma_j^z + \alpha(t) \, \sigma_j^x \right]$$
$$- \beta(t) \sum_{j,k} J_{j,k} \left[\sigma_j^z \sigma_k^z + \alpha(t) \, \sigma_j^x \sigma_k^x \right]. \quad (C2)$$

where $\beta(t)$ is function of $\alpha(t)$ as specified in Eq. (21).

We want to prepare the ground state of $H_{XZ} \equiv H_{\text{eff}}(1, 0) = -\beta \sum_{j,k} J_{j,k} \left(\sigma_j^z \sigma_k^z + \sigma_j^x \sigma_k^x \right)$. Hence we can first prepare the ground state of a ferromagnetic Ising Hamiltonian $H_{\text{Ising}} \equiv H_{\text{eff}}(0, h_0) = \beta \left(h_0 \sum_j \sigma_j^z - \sum_{j,k} J_{j,k} \sigma_j^z \sigma_k^z \right)$ which simply corresponds to the ferromagnetic state in which all the spins are polarized along z. Then the ground state of H_{XZ} is obtained by the adiabatic variation of the parameters $h/h_0 : 1 \rightarrow 0$ and $\alpha : 0 \rightarrow 1$.

An example of adiabatic preparation of the ground state of the Hamiltonian $H_{\text{eff}}(1, 0)$ is shown in Fig 8. The parameters α and h are varied according to (see the curves Fig. 8 (b))

$$h(t) = h_0 \, e^{-rt}$$
$$\alpha(t) = 1 - e^{-rt}. \quad (C3)$$

Initially the parameters can be varied rapidly because the corresponding gap between ground and first excited state is relatively large as depicted in Fig. 8 (a). As H_{eff} approaches the target Hamiltonian the gap reduces and correspondingly the variation have to slow down. The curves in Fig. 8 (c) are obtained by numerical integration of the Schrödinger Equation with the time dependent Hamiltonian (C2), and are equal to the dashed curves in Fig. 4 (a). The red, thin line in Fig. 8 (c) is the fidelity between the state obtained with the adiabatic evolution and the instantaneous ground state. This curve is very close to 1 at all times indicating that the system actually follows the adiabatic ground state. The spin-spin couplings that are used in these calculation are that discussed in Sec. III A 4. The Hamiltonian $H_{\text{eff}}(1, 0)$ with these coupling strengths exhibits long range entanglement, that is strong entanglement between first and last spin. This feature is described by the blue tick curve in Fig. 8 (c), that displays the entanglement, as measured by the concurrence between first and last spins. As expected, at large time the end spins are strongly entangled.

[1] R. Blatt and D. Wineland, Nature **453**, 1008 (2008).

[2] M. A. Nielsen and I. L. Chuang, *Quantum Computation and Quantum Information* (Cambridge U.P., ISBN = 0-521-63503-9, Cambridge, 2000)

[3] H. J. Kimble, Nature **453**, 1023 (2008).

[4] J. I. Cirac, P. Zoller, H. J. Kimble, and H. Mabuchi, Phys. Rev. Lett. **78**, 3221 (1997).

[5] S. Bose, Phys. Rev. Lett. **91**, 207901 (2003).

[6] J. Eisert, M. B. Plenio, S. Bose, and J. Hartley, Phys. Rev. Lett. **93**, 190402 (2004).

[7] B. Kraus and J. I. Cirac, Phys. Rev. Lett. **92**, 013602 (2004).

[8] S. Zippilli, G. A. Olivares-Rentera, G. Morigi, C. Schuck, F. Rohde, and J. Eschner, New J. Phys. **10**, 103003 (2008).

[9] J. B. Brask, I. Rigas, E. S. Polzik, U. L. Andersen, and A. S. Sørensen, Phys. Rev. Lett. **105**, 160501 (2010).

[10] W. J. Munro, K. A. Harrison, A. M. Stephens, S. J. Devitt, and K. Nemoto, Nature Photonics **4**, 792 (2010).

[11] A. Gonzalez-Tudela, D. Martin-Cano, E. Moreno, L. Martin-Moreno, C. Tejedor, and F. J. Garcia-Vidal, Phys. Rev. Lett. **106**, 020501 (2011).

[12] M. Leijnse and K. Flensberg, Phys. Rev. Lett. **107**, 210502 (2011).

[13] L. Banchi, A. Bayat, P. Verrucchi, and S. Bose, Phys. Rev. Lett. **106**, 140501 (2011).

[14] A. Wolf, G. De Chiara, E. Kajari, E. Lutz, and G. Morigi, Europhys. Lett. **95**, 60008 (2011).

[15] L. Trifunovic, O. Dial, M. Trif, J. R. Wootton, R. Abebe, A. Yacoby, and D. Loss, Phys. Rev. X **2**, 011006 (2012).

[16] S. Zippilli, M. Paternostro, G. Adesso, and F. Illuminati, Phys. Rev. Lett. **110**, 040503 (2013).

[17] L. Campos Venuti, C. Degli Esposti Boschi, and M. Roncaglia, Phys. Rev. Lett. **96**, 247206 (2006).

[18] L. Campos Venuti, S. M. Giampaolo, F. Illuminati, and P. Zanardi, Phys. Rev. A **76**, 052328 (2007).

[19] S. M. Giampaolo and F. Illuminati, Phys. Rev. A **80**, 050301(R) (2009).

[20] S. M. Giampaolo and F. Illuminati, New J. Phys. **12**, 025019 (2010).

[21] G. Gualdi, S. M. Giampaolo, and F. Illuminati, Phys. Rev. Lett. **106**, 050501 (2011).

[22] S. Zippilli, S. M. Giampaolo, and F. Illuminati, arXiv:1302.1205 (2013), and Phys. Rev. A, to appear.

[23] C. Schneider, D. Porras, and T. Schätz, Rep. Prog. Phys. **75**, 024401 (2012).

[24] A. Friedenauer, H. Schmitz, J. T. Glueckert, D. Porras, and T. Schätz, Nature Phys. **4**, 757 (2008).

[25] K. Kim, M.-S. Chang, S. Korenblit, R. Islam, E. E. Edwards, J. K. Freericks, G.-D. Lin, L.-M. Duan, and C. Monroe, Nature **465**, 590 (2010).

[26] R. Islam, E. E. Edwards, K. Kim, S. Korenblit, C. Noh, H. Carmichael, G.-D. Lin, L.-M. Duan, C.-C. Joseph Wang, J. K. Freericks, and C. Monroe, Nature Commun. **2**, 377 (2011).

[27] B. P. Lanyon, C. Hempel, D. Nigg, M. Müller, R. Gerritsma, F. Zähringer, P. Schindler, J. T. Barreiro, M. Rambach, G. Kirchmair, M. Hennrich, P. Zoller, R. Blatt, and C. F. Roos, Science **334**, 57 (2011).

[28] S. A. Schulz, U. Poschinger, F. Ziesel, and F.Schmidt-Kaler, New J. Phys. **10**, 045007 (2008).

[29] D. Kaufmann, T. Collath, M. T. Baig, P. Kaufmann, E. Asenwar, M. Johanning, and Ch. Wunderlich, Applied Physics B **107**, 935 (2012).

[30] F. Mintert and C. Wunderlich, Phys. Rev. Lett. **87**, 25 (2001).

[31] Ch. Wunderlich, in *Laser Physics at the Limit* (Springer, New York, 2002), p. 261.

[32] M. Johanning, A. F. Varon, and C. Wunderlich, J. Phys. B: At. Mol. Opt. Phys. **42**, 1 (2009).

[33] A. Khromova, C. Piltz, B. Scharfenberger, T. F. Gloger, M. Johanning, A. F. Varón, and Ch. Wunderlich, Phys. Rev. Lett. **108**,

220502 (2012).

[34] G. Breit and I. Rabi, Phys. Rev. **38**, 2082 (1931).

[35] S. Lloyd, Science **273**, 1073 (1996).

[36] H. Wunderlich, Ch. Wunderlich, K. Singer, and F. Schmidt-Kaler, Phys. Rev. A **79,** 052324 (2009)

[37] M. T. Baig *et al.*, to appear (2013).

[38] C. Ospelkaus, U. Warring, Y. Colombe, K. R. Brown, J. M. Amini, D. Leibfried, and D. J. Wineland, Nature **476**, 181 (2011).

[39] B. Scharfenberger *et al.*, to appear (2013).

[40] E. L. Hahn, Phys. Rev. **80**, 580 (1950).

[41] B. S. Piltz *et al.*, to appear (2013).

[42] N. Timoney, I. Baumgart, M. Johanning, A. F. Varón, Ch. Wunderlich, M. B. Plenio, and A. Retzker, Nature **476,** 185 (2011).

[43] N. Timoney, V. Elman, S. Glaser, C. Weiss, M. Johanning, W. Neuhauser, and Ch. Wunderlich, Phys. Rev. A **77**, 052334 (2008).

[44] A. Messiah *Quantum Mechanics* Vol. II (North Holland Publishing Company, Amsterdam, 1962).